Optimal Attitude Control of Spacecraft Using Pyramid-type CMGs

By Ryo SAITO[1)], Yasuhiro SHOJI[1)], Satoshi SATOH[1)] and Katsuhiko YAMADA[1)]

[1)]*Graduate School of Engineering, Osaka University, Osaka, Japan*

This paper proposes a new method for time optimal attitude control of spacecraft using Pyramid-type CMGs. In this method, the gimbal rates of the CMGs are determined only based on the time trajectories of the spacecraft attitude and the gimbal angles from the initial state to the target one. These trajectories are generated as a solution of an optimization problem to minimize the maneuvering time. Any “steering law” does not appear in the trajectory generating process, and thus, the singularity of the CMGs is not a problem in this method. In this paper, we formulate optimization problems for generating the trajectories, and show a specific control algorithm utilizing them. Finally, numerical simulations are performed to verify the usefulness of the proposed control method.

宇宙機のピラミッド配置型 CMG による最適姿勢制御

齋藤涼（阪大・院），莊司泰弘（阪大），佐藤訓志（阪大），山田克彦（阪大）

本研究では，ピラミッド配置型 CMG による宇宙機の時間最適姿勢制御の新たな手法を提案する．本手法において CMG のジンバル角速度は初期状態から目標状態に至る宇宙機の姿勢やジンバル角度の軌道によってのみ決定される．これらの軌道は姿勢変更時間を最小化するような最適化問題を解くことによって生成される．いかなる「ステアリング則」も，この軌道生成過程には登場しないため，提案手法においては CMG の特異点の存在は問題とならない．本稿では，軌道生成のための最適化問題を定式化し，それらを利用した具体的な制御アルゴリズムを示す．最後に，数値シミュレーションにより，提案手法の有用性を検証する．

Key Words: Spacecraft, Control Moment Gyro, Trajectry Generation, Optimal Control

Nomenclature

$\boldsymbol{J}$	:	inertia of spacecraft
$\boldsymbol{\omega}$	:	angular velocity of spacecraft
β	:	skew angle of Pyramid-type CMGs
h_{w}	:	magnitude of angular momentum of wheel
CMG$_k$	:	the kth CMG of Pyramid-type CMGs ($k = 1, 2, 3, 4$)
$\boldsymbol{h}_k$	:	angular momentum of CMG$_k$ ($k = 1, 2, 3, 4$)
θ_k	:	gimbal angle of CMG$_k$ ($k = 1, 2, 3, 4$)
T	:	maneuvering time

Subscripts

0	:	initial
f	:	final

1. Introduction

A momentum exchange actuator is useful for reorienting spacecraft, because it consumes only electric power in general, which can be replenished sustainably in space. A control moment gyro (CMG) is one of such devices. A CMG contains a gimballed wheel that spins at a large and constant speed, and its spin axis can be changed with respect to the spacecraft around its gimbal axis. Changing the spin axis generates a gyroscopic reaction torque orthogonal to both the wheel spin axis and the gimbal axis, and it is significantly amplified relative to the gimbal torque input. In practice, a CMG can output orders of magnitude higher torque for the power of an equivalent reaction wheel, [1)] which is another momentum exchange actuator.

A single-gimbal control moment gyro (SGCMG) has only one degree of freedom, and thus, three or more SGCMGs are generally used for the three-axis attitude control. However, there are some combinations of gimbal angles where the degree of freedom of the output torque becomes less than three and CMGs cannot generate torque in certain directions. [2)] In those singular states, the gimbal rates for desired torque cannot be obtained explicitly. Therefore, the singularity problem is a serious obstacle to construct of a steering law, which determines the gimbal angles from the desired torque explicitly. Although several authors have studied steering laws for avoiding the singularity problem, [3) 4) 5)] no complete solution has been proposed.

This paper proposes a new method for time optimal attitude control using Pyramid-type CMGs. In this method, the gimbal rates are determined only using time trajectories of the spacecraft attitude and the gimbal angles from the initial state to the target ones. These trajectories are generated as a solution of an optimization problem to minimize the maneuvering time under some capacity constraints of the CMGs. No “steering law” appears in the trajectory generation process, and thus, the singular problem does not exist any more in this method. Furthermore, the trajectories are updated repeatedly during the maneuver in order to eliminate the attitude and gimbal angle errors caused by disturbances.

In this paper, we first parametrize the trajectories with finite number of parameters using the method developed by Nishiyama et al. [6)] This method expresses each trajectory as a weighted sum of triangle wave functions, and the optimization problems for generating or updating the trajectories are formulated in the form of finite-dimensional optimization problems. Then, a specific control algorithm utilizing them is shown. Finally, numerical simulations of rest-to-rest attitude maneuver of a spacecraft are conducted in order to verify the usefulness of the proposed method.

2. Modeling

2.1. Pyramid-type CMGs

Consider a Pyramid-type CMG system which is composed of four SGCMGs arranged as shown in Fig. 1. The x, y, and z in Fig. 1 are the axes of the body-fixed frame $\mathcal{F}_\mathrm{b}$. The angular momentum of each SGCMG is expressed as follows:

$$\boldsymbol{h}_1 = h_\mathrm{w}\begin{bmatrix}-\sin\theta_1\cos\beta\\ \cos\theta_1\\ \sin\theta_1\sin\beta\end{bmatrix},\quad \boldsymbol{h}_2 = h_\mathrm{w}\begin{bmatrix}-\cos\theta_2\\ -\sin\theta_2\cos\beta\\ \sin\theta_2\sin\beta\end{bmatrix},$$
$$\boldsymbol{h}_3 = h_\mathrm{w}\begin{bmatrix}\sin\theta_3\cos\beta\\ -\cos\theta_3\\ \sin\theta_3\sin\beta\end{bmatrix},\quad \boldsymbol{h}_4 = h_\mathrm{w}\begin{bmatrix}\cos\theta_4\\ \sin\theta_4\cos\beta\\ \sin\theta_4\sin\beta\end{bmatrix}. \tag{1}$$

Assuming that each angular momentum of the gimbal rotation is negligibly small, the total momentum of the Pyramid-type CMGs, $\boldsymbol{h}_\mathrm{c}$, is given by

$$\boldsymbol{h}_\mathrm{c}(\boldsymbol{\theta}) = \sum_{k=1}^{4}\boldsymbol{h}_k(\theta_k) \tag{2}$$

where $\boldsymbol{\theta} = [\theta_1, \theta_2, \theta_3, \theta_4]^\mathrm{T}$. The attitude control torque $\boldsymbol{\tau}_\mathrm{c}$ by the CMGs is expressed in the following form:

$$\boldsymbol{\tau}_\mathrm{c} = -\dot{\boldsymbol{h}}_\mathrm{c} = -h_\mathrm{w}\boldsymbol{A}\dot{\boldsymbol{\theta}} \tag{3}$$

where the matrix $\boldsymbol{A}$ is a Jacobian matrix of $\boldsymbol{h}_\mathrm{c}/h_\mathrm{w}$, i.e. $\boldsymbol{A} = (1/h_\mathrm{w})\partial\boldsymbol{h}_\mathrm{c}/\partial\boldsymbol{\theta}$. The gimbal rates of the CMGs for the desired control torque, $\boldsymbol{\tau}_\mathrm{c}$, can be calculated directly from Eq. (3) as

$$\dot{\boldsymbol{\theta}} = -\frac{1}{h_\mathrm{w}}\boldsymbol{A}^\dagger\boldsymbol{\tau}_\mathrm{c} \tag{4}$$

where $\boldsymbol{A}^\dagger$ is the pseudo-inverse matrix of $\boldsymbol{A}$. In case the row rank of $\boldsymbol{A}$ is not full, $\boldsymbol{A}^\dagger$ cannot be calculated, and then the CMGs becomes singular.

2.2. Equations of Motion

In this subsection, it is assumed that the disturbance torque exerted on the spacecraft is zero, and that the total angular momentum of the spacecraft, $\boldsymbol{h}_\mathrm{s}$, is zero at the beginning of the control. By the angular momentum conservation, $\boldsymbol{h}_\mathrm{s}$ is conserved at zero during the maneuver, namely, the following relation holds:

$$\boldsymbol{h}_\mathrm{s} = \boldsymbol{J}\boldsymbol{\omega} + \boldsymbol{h}_\mathrm{c} = \boldsymbol{0}. \tag{5}$$

Accordingly, we obtain

$$\boldsymbol{\omega} = -\boldsymbol{J}^{-1}\boldsymbol{h}_\mathrm{c}. \tag{6}$$

The attitude of the spacecraft with respect to the inertial frame is expressed by Rodrigues parameters. Rodrigues parameters are defined by the axis of rotation $\hat{\boldsymbol{\alpha}}$ and the rotation angle ϕ as follows:

$$\boldsymbol{p} = \hat{\boldsymbol{\alpha}}\tan\frac{\phi}{2} \tag{7}$$

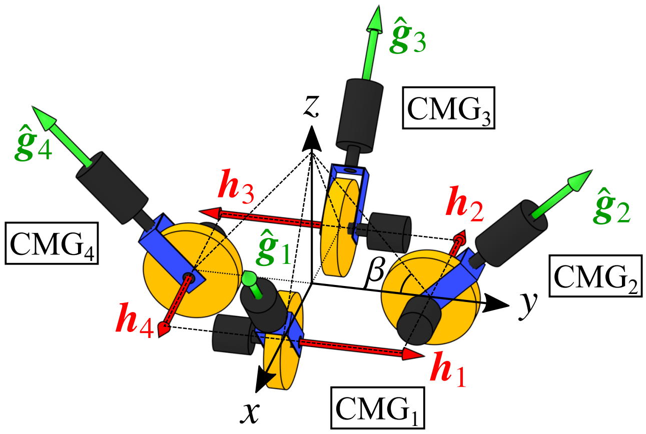

Fig. 1. Pyramid-type CMG System

where $\boldsymbol{p}$ is a 3×1 vector. The kinematic equation relating to the time derivative of Rodrigues parameters to the angular velocity of the spacecraft is given [7] as

$$\dot{\boldsymbol{p}} = \frac{1}{2}(\boldsymbol{I}_3 + \boldsymbol{p}^\times + \boldsymbol{p}\boldsymbol{p}^\mathrm{T})\boldsymbol{\omega} \tag{8}$$

where $\boldsymbol{p}^\times$ is the following skew symmetric matrix associated with the cross product of $\boldsymbol{p} = [p_1, p_2, p_3]^\mathrm{T}$:

$$\boldsymbol{p}^\times = \begin{bmatrix}0 & -p_3 & p_2\\ p_3 & 0 & -p_1\\ -p_2 & p_1 & 0\end{bmatrix}. \tag{9}$$

By substituting Eq. (6) into Eq. (8), we obtain the relationship between the gimbal angles of the CMGs and the Rodrigues parameters of the spacecraft as follows:

$$\dot{\boldsymbol{p}} = -\frac{1}{2}(\boldsymbol{I}_3 + \boldsymbol{p}^\times + \boldsymbol{p}\boldsymbol{p}^\mathrm{T})\boldsymbol{J}^{-1}\boldsymbol{h}_c(\boldsymbol{\theta}). \tag{10}$$

3. Time optimal attitude control

3.1. Outline of the proposed method

In the proposed method, the gimbal rates of the CMGs are determined from the time trajectories of the spacecraft attitude and the gimbal angles from the initial state to the target one. The outline of the proposed method is shown in Fig. 2.

As shown in Fig. 2, the control sequence is divided into two phases, Time Minimization Phase (TMP) and Error Minimization Phase (EMP). In the TMP, at first, the trajectories of the spacecraft attitude and the gimbal angles which realize time optimal transition of the attitude from the current one to the target one are calculated, and the CMGs are controlled based on them. If the gimbal angles are determined only by the first generated trajectories, the final attitude may be different from the target one due to modeling error, disturbance torque and so on. Therefore, the trajectories are updated repeatedly in order to eliminate errors at a fixed time interval Δt_u throughout the maneuver.

When the attitude of the spacecraft reaches near the target one, the trajectories cannot be updated because the optimization problem for updating the trajectories becomes infeasible. That is, before the state of the spacecraft reaches the target one completely, this control becomes unable to be continued, leaving errors. To reduce the errors, the control moves to the EMP, and

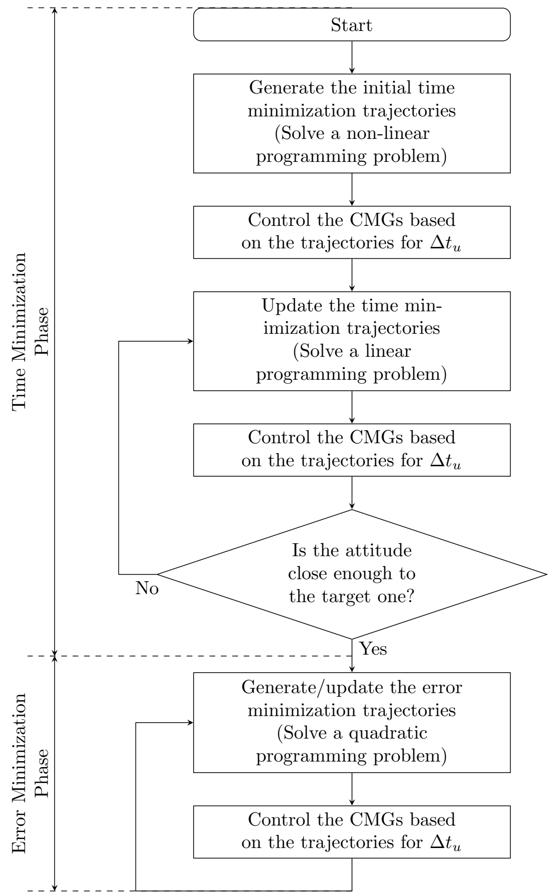

Fig. 2. Flowchart of the control sequence

the objective function of the optimization problem is changed from the maneuvering time to the errors of the spacecraft attitude and the gimbal angles.

In the following subsections, the optimization problems for generating or updating the trajectories are formulated. The pseudo-inverse matrix of the Jacobian matrix $\boldsymbol{A}$ is not used throughout the formulation process. Thus, even when the CMGs are in a singular state, the trajectories are generated or updated successfully, and the control can be continued.

3.2. Modeling of trajectories

In order to formulate the optimization problems in finite dimension, we set the trajectories with finite number of parameters. The trajectories of the gimbal rates of the CMGs, $\dot{\theta}_k$ $(k = 1, 2, 3, 4)$, and the second order time derivative of the Rodrigues parameters which represent the attitude of the spacecraft, $\ddot{\boldsymbol{p}} = [\ddot{p}_1, \ddot{p}_1, \ddot{p}_3]^{\mathrm{T}}$, are expressed as weighted sums of N triangle waves $\alpha_1(\tau), \ldots, \alpha_N(\tau)$ as follows:

$$\dot{\theta}_k(t; \boldsymbol{u}_k, T) = \sum_{i=1}^{N} u_{ki}\alpha_i\left(\tau(t; T)\right), \tag{11}$$

$$\ddot{p}_k(t; \boldsymbol{v}_k, T) = \sum_{i=1}^{N} v_{ki}\alpha_i\left(\tau(t; T)\right) \tag{12}$$

where $\boldsymbol{u}_k = [u_{k1}, \ldots, u_{kN}]^{\mathrm{T}}$, $\boldsymbol{v}_k = [v_{k1}, \ldots, v_{kN}]^{\mathrm{T}}$, and $\tau(t; T)$ is non-dimensional time defined by $\tau(t; T) = t/T$. The triangle waves $\alpha_1(\tau), \ldots, \alpha_N(\tau)$ are defined as follows:

$$\alpha_i(\tau) := \begin{cases} \frac{1}{\Delta\tau}(\tau - (\tau_{ci} - \Delta\tau)) & (\tau_{ci} - \Delta\tau \leq \tau \leq \tau_{ci}) \\ \frac{1}{\Delta\tau}((\tau_{ci} + \Delta\tau) - \tau) & (\tau_{ci} \leq \tau \leq \tau_{ci} + \Delta\tau) \\ 0 & \text{otherwise} \end{cases} \tag{13}$$

where

$$\tau_{ci} = (i-1)\Delta\tau, \quad \Delta\tau = \frac{1}{N-1} \quad (i = 1, \ldots, N). \tag{14}$$

The trajectories of the other quantities such as the gimbal angles θ_k $(k = 1, 2, 3, 4)$ and the Rodrigues parameters $\boldsymbol{p}$ are derived from the derivatives or integrals of Eqs. (11) and (12) as follows:

$$\ddot{\theta}_k(t; \boldsymbol{u}_k, T) = \frac{1}{T}\sum_{i=1}^{N} u_{ki}\xi_i\left(\tau(t; T)\right), \tag{15}$$

$$\theta_k(t; \boldsymbol{u}_k, T) = T\sum_{i=1}^{N} u_{ki}\hat{\beta}_i\left(\tau(t; T)\right) + \theta_{k0}, \tag{16}$$

$$\dot{p}_k(t; \boldsymbol{v}_k, T) = T\sum_{i=1}^{N} v_{ki}\hat{\beta}_i\left(\tau(t; T)\right) + \dot{p}_{k0}, \tag{17}$$

$$p_k(t; \boldsymbol{v}_k, T) = T^2\sum_{i=1}^{N} v_{ki}\hat{\gamma}_i\left(\tau(t; T)\right) + \dot{p}_{k0}t + p_{k0} \tag{18}$$

where $\hat{\beta}_i(\tau) = \beta_i(\tau) - \beta_i(0)$, $\hat{\gamma}_i(\tau) = \gamma_i(\tau) - \gamma_i(0) - \beta_i(0)\tau$,

$$\beta_i(\tau) = \int_{-\infty}^{\tau} \alpha_i(\tau')\mathrm{d}\tau', \tag{19}$$

$$\gamma_i(\tau) = \int_{-\infty}^{\tau} \beta_i(\tau')\mathrm{d}\tau', \tag{20}$$

$$\xi_i(\tau) = \frac{\mathrm{d}\alpha_i(\tau)}{\mathrm{d}\tau}. \tag{21}$$

3.3. Generating initial time minimization trajectories

At the beginning of the TMP, the initial time minimization trajectories are generated as a solution of a non-linear programming problem (NLP), which is formulated in this subsection.

Here, the following constraints are imposed on the gimbal rates and angular accelerations:

$$|\ddot{\theta}_k| \leq \ddot{\theta}_{\max}, \quad |\dot{\theta}_k| \leq \dot{\theta}_{\max} \quad (k = 1, 2, 3, 4). \tag{22}$$

These constraints (22) are equivalent to

$$\frac{1}{T\Delta\tau}|-u_{k,i} + u_{k,i+1}| \leq \ddot{\theta}_{\max} \quad (i = 1, \ldots, N-1), \tag{23}$$

$$|u_{k,i}| \leq \dot{\theta}_{\max} \quad (i = 1, \ldots, N). \tag{24}$$

To satisfy the initial and final conditions, the following boundary conditions are also imposed:

$$\dot{\boldsymbol{\theta}}(0; \bar{\boldsymbol{u}}, T) = \dot{\boldsymbol{\theta}}_0, \tag{25}$$

$$\dot{\boldsymbol{\theta}}(T; \bar{\boldsymbol{u}}, T) = \dot{\boldsymbol{\theta}}_f, \tag{26}$$

$$\boldsymbol{\theta}(T; \bar{\boldsymbol{u}}, T) = \boldsymbol{\theta}_f, \tag{27}$$

$$\boldsymbol{p}(T; \bar{\boldsymbol{v}}, T) = \boldsymbol{p}_f \tag{28}$$

where $\bar{\boldsymbol{u}} = [\boldsymbol{u}_1^{\mathrm{T}}, \ldots, \boldsymbol{u}_4^{\mathrm{T}}]^{\mathrm{T}}$ and $\bar{\boldsymbol{v}} = [\boldsymbol{v}_1^{\mathrm{T}}, \ldots, \boldsymbol{v}_3^{\mathrm{T}}]^{\mathrm{T}}$. Additionally, the trajectories have to satisfy the kinematic constraint in Eq.

(10). We consider this constraint only at fixed times t_i^K ($i = 1, \ldots, N^K$) defined by

$$t_i^K = \frac{T(i-1)}{N^K - 1}. \tag{29}$$

The trajectories are uniquely determined by $\bar{\boldsymbol{u}}$, $\bar{\boldsymbol{v}}$, and T. Therefore, the initial time minimization trajectories are obtained by solving the following optimization problem:

$$\begin{aligned} \min_{\bar{\boldsymbol{u}}, \bar{\boldsymbol{v}}, T} \quad & T \\ \text{subject to} \quad & T \geq 0,\ (23)\text{-}(28), \\ & (10) \text{ at } t = t_i^K\ (i = 1, \ldots, N^K). \end{aligned} \tag{30}$$

3.4. Trajectory updating

The optimization problem (30) is expected to take long time to be solved because it is an NLP, which cannot be guaranteed to be solved within a finite time. However, the trajectories need to be updated repeatedly at short intervals during the maneuver. Therefore, a quicker solution is necessary to update the trajectories. We introduce a linear programming problem (LP) as the linearization of the NLP (30). In general, linear programming problems can be solved efficiently within a finite time using a technique such as the simplex algorithm.

We denote the vector of optimization variables of the NLP (30) by $\boldsymbol{x}$, i.e. $\boldsymbol{x} = [\bar{\boldsymbol{u}}^{\mathrm{T}}, \bar{\boldsymbol{v}}^{\mathrm{T}}, T]^{\mathrm{T}}$. We linearize the NLP (30) around the constant vector $\boldsymbol{x}_0$, whose elements, $u_{ki,0}$ ($i = 1, \ldots, N,\ k = 1, 2, 3, 4$), $v_{ki,0}$ ($i = 1, \ldots, N,\ k = 1, 2, 3$), T_0, are defined by

$$u_{ki,0} = \dot{\theta}_k \left(\Delta t_{\mathrm{u}} + \frac{T_{\mathrm{latest}} - \Delta t_{\mathrm{u}}}{N-1}(i-1); \boldsymbol{u}_{k,\mathrm{latest}}, T_{\mathrm{latest}} \right), \tag{31}$$

$$v_{ki,0} = \ddot{p}_k \left(\Delta t_{\mathrm{u}} + \frac{T_{\mathrm{latest}} - \Delta t_{\mathrm{u}}}{N-1}(i-1); \boldsymbol{v}_{k,\mathrm{latest}}, T_{\mathrm{latest}} \right), \tag{32}$$

$$T_0 = T_{\mathrm{latest}} - \Delta t_{\mathrm{u}} \tag{33}$$

where the subscript $\cdot_{\mathrm{latest}}$ indicates the solution obtained in the latest calculation.

We rewrite the constraints (23) and (24) derived from the capacity of the CMGs as $\boldsymbol{c}^P(\boldsymbol{x}) \leq \boldsymbol{0}$. Similarly, the boundary conditions (25)-(28) and the kinematic constraints (10) at $t = t_i^K$ ($i = 1, \ldots, N^K$) are rewritten as $\boldsymbol{c}^B(\boldsymbol{x}) = \boldsymbol{0}$ and $\boldsymbol{c}^K(\boldsymbol{x}) = \boldsymbol{0}$, respectively. Then, $\boldsymbol{c}^P$, $\boldsymbol{c}^B$, $\boldsymbol{c}^K$ are linearized around $\boldsymbol{x} = \boldsymbol{x}_0$ into the following forms:

$$\left. \frac{\partial \boldsymbol{c}^P}{\partial \boldsymbol{x}} \right|_{\boldsymbol{x}_0} \Delta \boldsymbol{x} \leq -\boldsymbol{c}^P(\boldsymbol{x}_0), \tag{34}$$

$$\left. \frac{\partial \boldsymbol{c}^B}{\partial \boldsymbol{x}} \right|_{\boldsymbol{x}_0} \Delta \boldsymbol{x} = -\boldsymbol{c}^B(\boldsymbol{x}_0), \tag{35}$$

$$\left. \frac{\partial \boldsymbol{c}^K}{\partial \boldsymbol{x}} \right|_{\boldsymbol{x}_0} \Delta \boldsymbol{x} = -\boldsymbol{c}^K(\boldsymbol{x}_0) \tag{36}$$

where $\Delta \boldsymbol{x} = \boldsymbol{x} - \boldsymbol{x}_0$. Equations (34)-(36) are linear constraints with respect to $\Delta \boldsymbol{x}$. However, the constraint (36) is strict and sometimes makes the problem infeasible. To deal with this, we relax this equality constraint into an inequality one as follows:

$$\left| \left. \frac{\partial \boldsymbol{c}^K}{\partial \boldsymbol{x}} \right|_{\boldsymbol{x}_0} \Delta \boldsymbol{x} + \boldsymbol{c}^K(\boldsymbol{x}_0) \right| \leq \eta \left| \boldsymbol{c}^K(\boldsymbol{x}_0) \right| \tag{37}$$

where η is a relaxation factor and $|\cdot|$ is element-wise absolute value. Additionally, to prevent that the change of the trajectories become large, the following constraint is imposed:

$$|\Delta \bar{\boldsymbol{u}}| \leq \varepsilon \boldsymbol{1}_{4N} \tag{38}$$

where ε is a small positive real number and $\boldsymbol{1}_X$ is an X-dimensional vector of all ones. Then, the optimization problem (LP) for updating the trajectories is formulated as follows:

$$\begin{aligned} \min_{\Delta \boldsymbol{x}} \quad & \Delta T \\ \text{subject to} \quad & T_0 + \Delta T \geq 0,\ (34), (35), (37), (38). \end{aligned} \tag{39}$$

3.5. Generating/updating error minimization trajectories

As T_0 approaches zero, the LP (39) becomes infeasible and the time minimization trajectories cannot be updated. To cope with it, the control is switched to the EMP to converge the error to zero. In this phase, the error minimization trajectories, which realize the minimization of the attitude and gimbal angle errors, are generated and updated by solving the optimization problem formulated in this subsection. This problem is also to be solved at short intervals during the maneuver as the LP (39), thus it is formulated in the form of a quadratic programming problem (QP).

First, the maneuver completion time T is fixed at $T = T_{\mathrm{h}}$, and the objective function is defined as follows:

$$\sum_{i=1}^{N^Q} \left(\|\boldsymbol{e}_\theta(t_i^Q; \bar{\boldsymbol{u}})\|^2 + \mu \|\boldsymbol{e}_p(t_i^Q; \bar{\boldsymbol{v}})\|^2 \right) \tag{40}$$

where $\boldsymbol{e}_\theta(t; \bar{\boldsymbol{u}}) = \boldsymbol{\theta}(t; \bar{\boldsymbol{u}}, T_{\mathrm{h}}) - \boldsymbol{\theta}_f$, $\boldsymbol{e}_p(t; \bar{\boldsymbol{v}}) = \boldsymbol{p}(t; \bar{\boldsymbol{v}}, T_{\mathrm{h}}) - \boldsymbol{p}_f$, and μ is a positive real number. t_i^Q ($i = 1, \ldots, N^Q$) are discrete time defined by

$$t_i^Q = \frac{T_{\mathrm{h}}(i-1)}{N^Q - 1}. \tag{41}$$

Let $\boldsymbol{\theta}_k$ ($k = 1, 2, 3, 4$) and $\boldsymbol{p}_k$ ($k = 1, 2, 3$) be

$$\boldsymbol{\theta}_k = [\theta_k(t_1^Q; \boldsymbol{u}_k, T_{\mathrm{h}}), \ldots, \theta_k(t_{N^Q}^Q; \boldsymbol{u}_k, T_{\mathrm{h}})]^{\mathrm{T}}, \tag{42}$$

$$\boldsymbol{p}_k = [p_k(t_1^Q; \boldsymbol{v}_k, T_{\mathrm{h}}), \ldots, p_k(t_{N^Q}^Q; \boldsymbol{v}_k, T_{\mathrm{h}})]^{\mathrm{T}}. \tag{43}$$

They can be expressed as follows:

$$\boldsymbol{\theta}_k = T_{\mathrm{h}} \boldsymbol{B} \boldsymbol{u}_k + \theta_{k0} \boldsymbol{1}_{N^Q}, \tag{44}$$

$$\boldsymbol{p}_k = T_{\mathrm{h}}^2 \boldsymbol{\Gamma} \boldsymbol{v}_k + \dot{p}_{k0} \boldsymbol{t}^Q + p_{k0} \boldsymbol{1}_{N^Q} \tag{45}$$

where $\boldsymbol{t}^Q = [t_1^Q, \ldots, t_{N^Q}^Q]^{\mathrm{T}}$. $\boldsymbol{B} = [B_{ij}] \in \mathbb{R}^{N^Q \times N}$, $\boldsymbol{\Gamma} = [\Gamma_{ij}] \in \mathbb{R}^{N^Q \times N}$ are the matrices whose elements are defined by

$$B_{ij} = \hat{\beta}_j(t_i^Q / T_{\mathrm{h}}), \quad \Gamma_{ij} = \hat{\gamma}_j(t_i^Q / T_{\mathrm{h}}). \tag{46}$$

Furthermore, let $\bar{\boldsymbol{\theta}} = [\boldsymbol{\theta}_1^{\mathrm{T}}, \ldots, \boldsymbol{\theta}_4^{\mathrm{T}}]^{\mathrm{T}}$, $\bar{\boldsymbol{p}} = [\boldsymbol{p}_1^{\mathrm{T}}, \ldots, \boldsymbol{p}_3^{\mathrm{T}}]^{\mathrm{T}}$. They can be expressed as follows:

$$\bar{\boldsymbol{\theta}} = T_{\mathrm{h}} \bar{\boldsymbol{B}} \bar{\boldsymbol{u}} + \bar{\boldsymbol{\theta}}_{\mathrm{c}}, \tag{47}$$

$$\bar{\boldsymbol{p}} = T_{\mathrm{h}}^2 \bar{\boldsymbol{\Gamma}} \bar{\boldsymbol{v}} + \bar{\boldsymbol{p}}_{\mathrm{c}} \tag{48}$$

where $\bar{\boldsymbol{B}} = \text{block-diag}[\boldsymbol{B}, \boldsymbol{B}, \boldsymbol{B}, \boldsymbol{B}]$, $\bar{\boldsymbol{\Gamma}} = \text{block-diag}[\boldsymbol{\Gamma}, \boldsymbol{\Gamma}, \boldsymbol{\Gamma}]$. Also, $\bar{\boldsymbol{\theta}}_{\mathrm{c}}$ and $\bar{\boldsymbol{p}}_{\mathrm{c}}$ are:

$$\bar{\boldsymbol{\theta}}_{\mathrm{c}} = \begin{bmatrix} \theta_{10} \boldsymbol{1}_{N^Q} \\ \vdots \\ \theta_{40} \boldsymbol{1}_{N^Q} \end{bmatrix}, \quad \bar{\boldsymbol{p}}_{\mathrm{c}} = \begin{bmatrix} \dot{p}_{10} \boldsymbol{t}_Q + p_{10} \boldsymbol{1}_{N^Q} \\ \vdots \\ \dot{p}_{30} \boldsymbol{t}_Q + p_{30} \boldsymbol{1}_{N^Q} \end{bmatrix}. \tag{49}$$

The target values of $\bar{\boldsymbol{\theta}}$ and $\bar{\boldsymbol{p}}$ are denoted as $\bar{\boldsymbol{\theta}}_f$ and $\bar{\boldsymbol{p}}_f$, respectively, that is,

$$\bar{\boldsymbol{\theta}}_f = [\theta_{1f}\mathbf{1}_{NQ}^{\mathrm{T}}, \ldots, \theta_{4f}\mathbf{1}_{NQ}^{\mathrm{T}}]^{\mathrm{T}}, \tag{50}$$

$$\bar{\boldsymbol{p}}_f = [p_{1f}\mathbf{1}_{NQ}^{\mathrm{T}}, \ldots, p_{3f}\mathbf{1}_{NQ}^{\mathrm{T}}]^{\mathrm{T}}. \tag{51}$$

Let $\bar{\boldsymbol{e}}_\theta = \bar{\boldsymbol{\theta}} - \bar{\boldsymbol{\theta}}_f$, $\bar{\boldsymbol{e}}_p = \bar{\boldsymbol{p}} - \bar{\boldsymbol{p}}_f$, and $\bar{\boldsymbol{e}} = [\bar{\boldsymbol{e}}_\theta^{\mathrm{T}}, \sqrt{\mu}\bar{\boldsymbol{e}}_p^{\mathrm{T}}]^{\mathrm{T}}$, and then the objective function (40) can be rewritten as follows:

$$\bar{\boldsymbol{e}}_\theta^{\mathrm{T}}\bar{\boldsymbol{e}}_\theta + \mu\bar{\boldsymbol{e}}_p^{\mathrm{T}}\bar{\boldsymbol{e}}_p = \bar{\boldsymbol{e}}^{\mathrm{T}}\bar{\boldsymbol{e}}. \tag{52}$$

From Eqs. (47) and (48), $\bar{\boldsymbol{e}}$ can be expressed as

$$\bar{\boldsymbol{e}} = \boldsymbol{P}\boldsymbol{y} + \boldsymbol{q} \tag{53}$$

where $\boldsymbol{y} = [\bar{\boldsymbol{u}}^{\mathrm{T}}, \bar{\boldsymbol{v}}^{\mathrm{T}}]^{\mathrm{T}}$,

$$\boldsymbol{P} = \begin{bmatrix} T_{\mathrm{h}}\bar{\boldsymbol{B}} & \mathbf{0} \\ \mathbf{0} & \sqrt{\mu}T_{\mathrm{h}}^2\bar{\boldsymbol{\Gamma}} \end{bmatrix}, \quad \boldsymbol{q} = \begin{bmatrix} \bar{\boldsymbol{\theta}}_{\mathrm{c}} - \bar{\boldsymbol{\theta}}_f \\ \sqrt{\mu}(\bar{\boldsymbol{p}}_{\mathrm{c}} - \bar{\boldsymbol{p}}_f) \end{bmatrix}. \tag{54}$$

Therefore, the objective function $\bar{\boldsymbol{e}}^{\mathrm{T}}\bar{\boldsymbol{e}}$ can be rewritten as follows:

$$\begin{aligned} \bar{\boldsymbol{e}}^{\mathrm{T}}\bar{\boldsymbol{e}} &= (\boldsymbol{P}\boldsymbol{y} + \boldsymbol{q})^{\mathrm{T}}(\boldsymbol{P}\boldsymbol{y} + \boldsymbol{q}) \\ &= \boldsymbol{y}^{\mathrm{T}}\boldsymbol{P}^{\mathrm{T}}\boldsymbol{P}\boldsymbol{y} + 2\boldsymbol{q}^{\mathrm{T}}\boldsymbol{P}\boldsymbol{y} + \text{const.} \\ &= (\boldsymbol{y}_0 + \Delta\boldsymbol{y})^{\mathrm{T}}\boldsymbol{P}^{\mathrm{T}}\boldsymbol{P}(\boldsymbol{y}_0 + \Delta\boldsymbol{y}) \\ &\quad + 2\boldsymbol{q}^{\mathrm{T}}\boldsymbol{P}(\boldsymbol{y}_0 + \Delta\boldsymbol{y}) + \text{const.} \\ &= \Delta\boldsymbol{y}^{\mathrm{T}}\boldsymbol{P}^{\mathrm{T}}\boldsymbol{P}\Delta\boldsymbol{y} + 2[\boldsymbol{P}^{\mathrm{T}}(\boldsymbol{P}\boldsymbol{y}_0 + \boldsymbol{q})]\Delta\boldsymbol{y} + \text{const.} \end{aligned} \tag{55}$$

where $\boldsymbol{y}_0$ is a constant vector and $\Delta\boldsymbol{y} = \boldsymbol{y} - \boldsymbol{y}_0$. Let $\boldsymbol{H} = \boldsymbol{P}^{\mathrm{T}}\boldsymbol{P}, \boldsymbol{f} = 2[\boldsymbol{P}^{\mathrm{T}}(\boldsymbol{P}\boldsymbol{y}_0 + \boldsymbol{q})]$ and ignore the constant. Then, the objective function is rewritten in the form of a quadratic function with respect to $\Delta\boldsymbol{y}$ as follows:

$$\Delta\boldsymbol{y}^{\mathrm{T}}\boldsymbol{H}\Delta\boldsymbol{y} + \boldsymbol{f}^{\mathrm{T}}\Delta\boldsymbol{y}. \tag{56}$$

Next, the capacity constraints of the CMGs (23), (24), the initial condition (25), and the kinematic constraints ((10) at $t = t_i^K$ $(i = 1, \ldots, N^K)$) are considered. Note that the final conditions (26)-(28) are excluded. These constraints are linearized in the same way as Eqs. (34), (35), and (37), around the constant vector $\boldsymbol{y}_0$, whose elements, $u_{ki,0}$ $(i = 1, \ldots, N,\ k = 1, 2, 3, 4)$, $v_{ki,0}$ $(i = 1, \ldots, N,\ k = 1, 2, 3)$, are defined by

$$u_{ki,0} = \dot{\theta}_k\left(\Delta t_{\mathrm{u}} + \frac{T_{\mathrm{h}}}{N-1}(i-1); \boldsymbol{u}_{k,\mathrm{latest}}, T_{\mathrm{latest}}\right), \tag{57}$$

$$v_{ki,0} = \ddot{p}_k\left(\Delta t_{\mathrm{u}} + \frac{T_{\mathrm{h}}}{N-1}(i-1); \boldsymbol{v}_{k,\mathrm{latest}}, T_{\mathrm{latest}}\right). \tag{58}$$

Let the capacity constraints, the initial condition, and the kinematic constraints be $\boldsymbol{c}_{\mathrm{q}}^P(\boldsymbol{y}) \leq \mathbf{0}, \boldsymbol{c}_{\mathrm{q}}^B(\boldsymbol{y}) = \mathbf{0}$, and $\boldsymbol{c}_{\mathrm{q}}^K(\boldsymbol{y}) = \mathbf{0}$, respectively. Then, the linearized constraints can be expressed as follows:

$$\left.\frac{\partial \boldsymbol{c}_{\mathrm{q}}^P}{\partial \boldsymbol{y}}\right|_{\boldsymbol{y}_0} \Delta\boldsymbol{y} \leq -\boldsymbol{c}_{\mathrm{q}}^P(\boldsymbol{y}_0), \tag{59}$$

$$\left.\frac{\partial \boldsymbol{c}_{\mathrm{q}}^B}{\partial \boldsymbol{y}}\right|_{\boldsymbol{y}_0} \Delta\boldsymbol{y} = -\boldsymbol{c}_{\mathrm{q}}^B(\boldsymbol{y}_0), \tag{60}$$

$$\left|\left.\frac{\partial \boldsymbol{c}_{\mathrm{q}}^K}{\partial \boldsymbol{y}}\right|_{\boldsymbol{y}_0} \Delta\boldsymbol{y} + \boldsymbol{c}_{\mathrm{q}}^K(\boldsymbol{y}_0)\right| \leq \eta\left|\boldsymbol{c}_{\mathrm{q}}^K(\boldsymbol{y}_0)\right|. \tag{61}$$

Additionally, the constraint (38) is also imposed for the same reason as the LP (39).

From the above, the QP for generating and updating the error minimization trajectories is formulated as follows:

$$\begin{aligned} \min_{\Delta\boldsymbol{y}} \quad & \Delta\boldsymbol{y}^{\mathrm{T}}\boldsymbol{H}\Delta\boldsymbol{y} + \boldsymbol{f}^{\mathrm{T}}\Delta\boldsymbol{y} \\ \text{subject to} \quad & (38), (59), (60), (61). \end{aligned} \tag{62}$$

3.6. Control algorithm

The proposed control algorithm is shown below.

Algorithm 1

(*Time Minimization Phase*)

- **Step 1:** Observe the current values of $\boldsymbol{\theta}$, $\dot{\boldsymbol{\theta}}$, $\boldsymbol{p}$, and $\dot{\boldsymbol{p}}$, then set $\boldsymbol{\theta}_0 \leftarrow \boldsymbol{\theta}$, $\dot{\boldsymbol{\theta}}_0 \leftarrow \dot{\boldsymbol{\theta}}$, $\boldsymbol{p}_0 \leftarrow \boldsymbol{p}$, and $\dot{\boldsymbol{p}}_0 \leftarrow \dot{\boldsymbol{p}}$.
- **Step 2:** Calculate the solution $\boldsymbol{x}^*$ of the NLP (30).
- **Step 3:** Set $\boldsymbol{x} \leftarrow \boldsymbol{x}^*$ and start the timer.
- **Step 4:** Control the CMGs based on the gimbal angle velocity trajectories set by the parameter $\boldsymbol{x}$ for Δt_{u}.
- **Step 5:** Observe the current values of $\boldsymbol{\theta}$, $\dot{\boldsymbol{\theta}}$, $\boldsymbol{p}$, and $\dot{\boldsymbol{p}}$, then set $\boldsymbol{\theta}_0 \leftarrow \boldsymbol{\theta}$, $\dot{\boldsymbol{\theta}}_0 \leftarrow \dot{\boldsymbol{\theta}}$, $\boldsymbol{p}_0 \leftarrow \boldsymbol{p}$, and $\dot{\boldsymbol{p}}_0 \leftarrow \dot{\boldsymbol{p}}$.
- **Step 6:** Calculate the solution $\Delta\boldsymbol{x}^*$ of the LP (39). If the LP is infeasible, set $\Delta\boldsymbol{x}^* \leftarrow \mathbf{0}$.
- **Step 7:** Set $\boldsymbol{x} \leftarrow \boldsymbol{x}_0 + \Delta\boldsymbol{x}^*$ and reset the time t to zero.
- **Step 8:** If T in $\boldsymbol{x}$ is greater than T_{th}, go back to Step 4.
- **Step 9:** Control the CMGs based on the gimbal angle velocity trajectories set by the parameter $\boldsymbol{x}$ until $t = T$.

(*Error Minimization Phase*)

- **Step 10:** Fix T as $T = T_{\mathrm{h}}$.
- **Step 11:** Observe the current values of $\boldsymbol{\theta}$, $\dot{\boldsymbol{\theta}}$, $\boldsymbol{p}$, and $\dot{\boldsymbol{p}}$, then set $\boldsymbol{\theta}_0 \leftarrow \boldsymbol{\theta}$, $\dot{\boldsymbol{\theta}}_0 \leftarrow \dot{\boldsymbol{\theta}}$, $\boldsymbol{p}_0 \leftarrow \boldsymbol{p}$, and $\dot{\boldsymbol{p}}_0 \leftarrow \dot{\boldsymbol{p}}$.
- **Step 12:** Calculate the solution $\Delta\boldsymbol{y}^*$ of the QP (62). If the QP is infeasible or the objective function value at the solution is positive, set $\Delta\boldsymbol{y}^* \leftarrow \mathbf{0}$.
- **Step 13:** Set $\boldsymbol{x} \leftarrow [\boldsymbol{y}_0^{\mathrm{T}}, T_{\mathrm{h}}]^{\mathrm{T}} + [(\Delta\boldsymbol{y}^*)^{\mathrm{T}}, 0]^{\mathrm{T}}$ and reset the time t to zero.
- **Step 14:** Control the CMGs based on the gimbal angle velocity trajectories set by the parameter $\boldsymbol{x}$ for Δt_{u}.
- **Step 15:** Go back to Step 11.

4. Numerical Simulations

In this section, the proposed control method is evaluated through numerical simulations of rest-to-rest attitude maneuver of a spacecraft.

The moment of inertia of the spacecraft, $\boldsymbol{J}$, in the body-fixed frame, the modeling error of the moment of inertia, $\boldsymbol{J}_{\mathrm{error}}$, in the body-fixed frame, the skew angle of the CMGs, β, and the magnitude of angular momentum of the wheel h_{w} are given by

$$\begin{aligned} \boldsymbol{J} &= \mathrm{diag}[10, 10, 10]\ [\mathrm{kgm}^2], \\ \boldsymbol{J}_{\mathrm{error}} &= \begin{bmatrix} 0.4 & 0.5 & 0.2 \\ 0.5 & -0.1 & 0.4 \\ 0.2 & 0.4 & 0.3 \end{bmatrix} [\mathrm{kgm}^2], \\ \beta &= 45\ [\mathrm{deg}],\ h_{\mathrm{w}} = 1\ [\mathrm{Nms}]. \end{aligned}$$

The true moment of inertia, $\boldsymbol{J}_{\mathrm{t}}$, is $\boldsymbol{J}_{\mathrm{t}} = \boldsymbol{J} + \boldsymbol{J}_{\mathrm{error}}$. The upper bound of the magnitudes of gimbal angular acceleration and velocity are set as

$$\ddot{\theta}_{\max} = 5\ [\mathrm{rad/s^2}],\ \dot{\theta}_{\max} = 1\ [\mathrm{rad/s}].$$

The parameters of the control algorithm are shown in Table 1. The initial and target states are selected as

$$\dot{\boldsymbol{\theta}}_0 = [0,0,0,0]^{\mathrm{T}},\quad \boldsymbol{\theta}_0 = [0,0,0,0]^{\mathrm{T}},\quad \boldsymbol{p}_0 = [0,0,0]^{\mathrm{T}},$$
$$\dot{\boldsymbol{\theta}}_f = [0,0,0,0]^{\mathrm{T}},\quad \boldsymbol{\theta}_f = [0,0,0,0]^{\mathrm{T}},\quad \boldsymbol{p}_f = \hat{\boldsymbol{\alpha}} \tan\frac{\phi}{2}.$$

The simulations are performed in two cases. For each case, the rotation axis $\hat{\boldsymbol{\alpha}}$ and angle ϕ are shown in Table 2.

Table 1. Parameter of control algorithm

Parameters	**Values**
N	30 (TMP), 10 (EMP)
N^K	$2N-1$
N^Q	$16N-15$
η	0.3
ε	0.2
μ	250
T_{h}	1.5 s
T_{th}	0.3 s
Δt_{u}	0.1 s

Table 2. Simulation cases

	$\hat{\boldsymbol{\alpha}}$	ϕ
Case 1	$[1,0,0]^{\mathrm{T}}$	20 deg
Case 2	$\frac{1}{\sqrt{3}}[1,1,1]^{\mathrm{T}}$	20 deg

The simulation results in *Case 1* and in *Case 2* are shown in Figs. 3 and 4, respectively. Figure 3(a) shows the gimbal rates of the CMGs where the two black horizontal broken lines indicate upper and lower constraints. Figure 3(b) shows the gimbal angles. Figure 3(c) shows the attitude of the spacecraft represented by Rodrigues parameters where the broken lines indicate the target values. Figure 3(d) shows the singularity of the CMGs, which is calculated as $\det(\boldsymbol{A}\boldsymbol{A}^{\mathrm{T}})$ and becomes small when the CMGs are near a singular state, and zero when the CMGs are completely in a singular state. The black vertical lines in these figures show the boundary between TMP and EMP. Figures 4(a), (b), (c), and (d) have the same meaning as above. As shown in Fig. 3, in *Case 1*, although the CMG is in a singular state around $t = 2$ s, both of the attitude of the spacecraft and the gimbal angles of the CMG reach the target values. The control is also performed properly in *Case 2* as shown in Fig. 4.

Figures 5 and 6 show the attitude errors $\|\boldsymbol{p} - \boldsymbol{p}_f\|$ in *Case 1* and *Case 2*, respectively. In each of the figures, (i) and (ii) show the attitude errors in the following cases:

(i) [*NLP* + *LP* + *QP*] The CMGs are controlled completely based on the proposed method (Algorithm 1).
(ii) [*only NLP*] Trajectory updating by solving the LP (39) or the QP (62) is not executed. That is, the initial time optimal trajectories from the NLP (30) is used throughout the control.

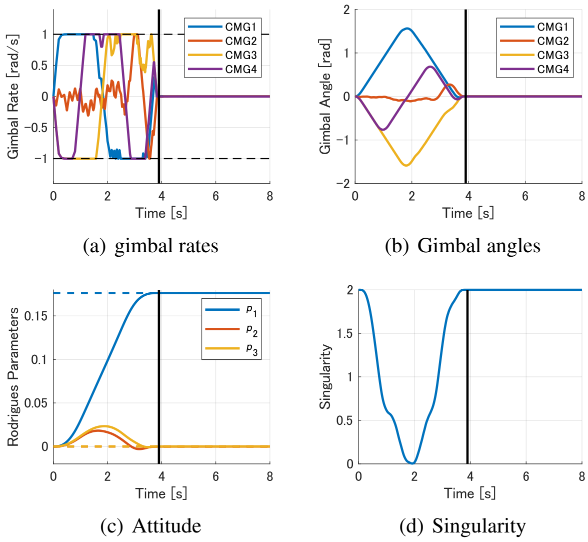

(a) gimbal rates (b) Gimbal angles
(c) Attitude (d) Singularity

Fig. 3. Simulation results in *Case 1*

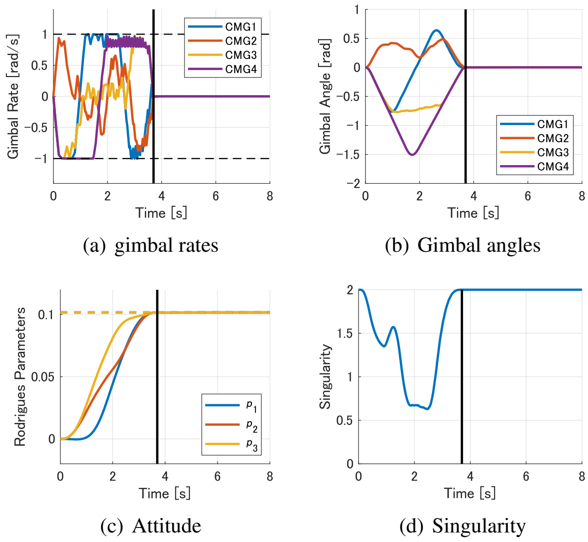

(a) gimbal rates (b) Gimbal angles
(c) Attitude (d) Singularity

Fig. 4. Simulation results in *Case 2*

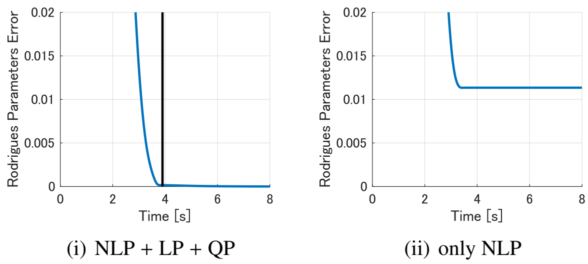

(i) NLP + LP + QP (ii) only NLP

Fig. 5. Attitude error in *Case 1*

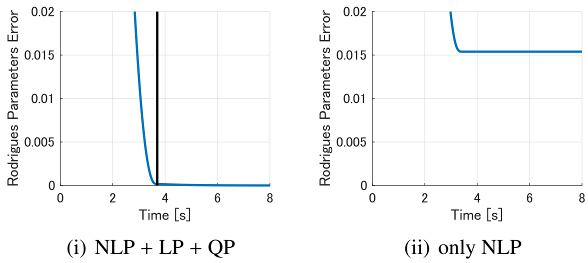

(i) NLP + LP + QP (ii) only NLP

Fig. 6. Attitude error in *Case 2*

As shown in Figs. 5 and 6, the attitude error remains due to the modeling error of the inertia $\boldsymbol{J}_{\mathrm{error}}$ when the trajectories are not updated, whereas the error is eliminated when the trajectories are updated both in *Case 1* and in *Case 2*.

5. Conclusion

In this paper, the time optimal control of the Pyramid-type CMGs is considered. The proposed method is composed of the two phases, Time Minimization Phase (TMP) and Error Minimization Phase (EMP). The maneuvering time is minimized in TMP, and the error remaining from TMP is eliminated in EMP. In both phases, the gimbal rates are determined based on time trajectories of them generated previously. The trajectories are updated repeatedly throughout the maneuver in order to eliminate the attitude error due to disturbances. By parametrization of the trajectories using triangle wave functions, the optimization problems for generating and updating them are formulated in the form of finite-dimensional optimization problems. The numerical simulation results show that the CMGs are controlled properly by the proposed method even when the CMGs become in a singular state, and the usefulness of the proposed method is verified.

References

1) Carpenter, M. D. and Peck, M. A. : Dynamics of a High-Agility, Low-Power Imaging Payload, *IEEE Trans. Robot.*, **24:3** (2008), pp. 666-675.
2) Wie, B. : Singularity Analysis and Visualization for Single-Gimbal Control Moment Gyro Systems, *Journal of Guidance, Control, and Dynamics*, **27:2** (2004), pp. 271-282.
3) Ford, K. A. and Hall, C. D. : Singular Direction Avoidance Steering for Control-Moment Gyros, *Journal of Guidance, Control, and Dynamics*, **23:4** (2000), pp.648-656.
4) Bedrosion, N. S., Paradiso, J., Bergmann, E. V., and Rowell, D. : Steering law design for redundant single-gimbal control moment gyroscopes, *Journal of Guidance, Control, and Dynamics*, **13:6** (1990), pp.1083-1089.
5) Tekinalp, O. and Yavuzoglu, E. : A new steering law for redundant control moment gyroscope clusters, *Aerospace Science and Technology*, **9** (2005), pp. 626-634.
6) Nishiyama, T., Yamada, K. and Yoshikawa, S. : A New Method for Motion Planning of Rotating Bodies under Multiple Constraints, *Trans. JSASS Space Tech. Japan*, **7:ists26** (2009), pp. Pd_7-Pd_16.
7) Shustr, M. D. : A Survey of Attitude Representations, *Journal of the Astronautical Sciences*, **41:4** (1993), pp. 439-517.